

Influence of Loading on the Mechanical Response of Linked Structures of Two Steels: A Numerical Study

Prashant P. Gargh¹, T. S. Srivatsan^{1,*} and Shivakumar Sastry²

¹Department of Mechanical Engineering, The University of Akron, Akron, Ohio 44325, USA

²Department of Electrical Engineering, The University of Akron, Akron, Ohio 44325, USA

Abstract: Two different sizes of the perforations in a metal sheet were chosen resulting essentially in a structure that was held together by links of varying thickness. A perforated sheet of the chosen metal was held together by thin links, while another was held together by thick links. The two designs of the perforated metal sheet were made possible using ABAQUS [version 6.13.2]. The specific metal chosen for this study was two steels having varying degree of high strength, i.e., an alloy steel and a carbon steel. The method of finite elements in synergism with a numerical approach was used to analyze the mechanical response of the perforated metal sheets when subjected to the influence of an external mechanical stimulus, such as, load that is applied in tension. For five different levels of the applied load, as a function of yield load of the candidate steel, the stresses, strains and resultant displacements induced in both the links and at nodal points were systematically determined. With the aid of numerical analysis, the mechanical behavior of the chosen steel structure, which was held together by a network of links, was systematically studied under the influence of an external mechanical stimulus, i.e., applied load. For each situation, i.e., thin links and thick links, the response kinetics under the influence of an external load was determined for the case of both symmetric loading and asymmetric loading.

Keywords: Alloy steel, carbon steel, perforated metal sheet, thin links, thick links, loading, nodes, displacement.

1. INTRODUCTION

The simple tension test has been traditionally used in the domain spanning engineering as a viable and useful method for the purpose of evaluating strength of a material, to include both yield strength and ultimate tensile strength. The two strengths are often referred by traditional design engineers and mechanical engineers as mechanical properties of the candidate material. The tension test has been used for the purpose of certifying and comparing different materials so as to determine their capacity for withstanding load without the occurrence of failure by fracture.

Perforated metal sheets are of interest in situations when it comes to the selection and use of a complete sheet of metal for a specific application. With the aid of conventional techniques, it is possible to manufacture a perforated metal sheet or a linked metal structure. In the prevailing era and commensurate with noticeable advances in the domain enveloping manufacturing techniques, a variety of perforations are available. This aids in the metal sheet or metal plate to have an impressive look while concurrently revealing a trend that is commensurate with advances in design [1-6]. Various features that a perforated metal sheet can possess besides an attractive appearance are the following: (i) light in weight, (ii) resistant to corrosion,

and (iii) a large open area, which is conducive for the passage of air or appropriate fluid medium. These plates can be manufactured in a variety of gage lengths using prevailing manufacturing techniques that are currently in widespread use in the engineering industry. Depending on the metal chosen, the overall strength-to-weight ratio is relatively good. A perforated metal sheet offers numerous applications where it can be put to effective use. A preliminary study on aspects related to mechanical behavior and resultant selection and use of perforated metal sheets was initially proposed by Goldberg and Jabbour [7] using an analytical method. Their study was conducted for the purpose of investigating the displacements experienced by a perforated metal sheet using field equations based on classical elastic theory. Another important outcome resulting from the study of Goldberg and Jabbour was that both the principal stress and principal strain at each and every point in the metal plate could be obtained using the general solution for a stress field when subjected to an external mechanical stimulus. The values that were obtained using the general solution were observed to converge faster to the values based on use of the elastic theory. Subsequently, Yettram and Awadalla [8] using the finite element technique put forth a method for the elastic stability of metal plates having a pattern of rectangular perforations, using the finite element technique. Their approach helped in providing an understanding of the method used for the prediction of buckling load and the resultant computational technique was considered to be easy, effective, reliable and safe. Another important concern with specific reference to practical applications

*Address correspondence to this author at the Department of Mechanical Engineering, The University of Akron, Akron, Ohio 44325, USA; Tel: 330-972-6196; Fax: 330-972-6027; E-mail: tsrivatsan@uakron.edu

was the bending experienced by the perforated metal plates, or sheets, having a pattern of square perforations; the elastic constants were obtained under conditions of bending. In his independent study, Fort [9] justified the solution obtained was capable of determining the stress distribution at all nodes for a perforated metal plate that was subjected to both symmetric bending and asymmetric bending. The metal plate, on account of 'local' stress concentration(s) arising from the presence of perforated regions, did develop a transverse shear stress that exerted an influence on both the stress components developed in an element, and the overall deformation experienced by an element in the plate. In a subsequent study, Yettram and Brown [10] presented and discussed the influence of stress distribution, under conditions of plane stress, on the nature of buckling load experienced by a perforated metal plate. Their method provided for an understanding that depending upon size and shape of the perforation in a chosen metal plate, and prevailing boundary conditions, the mode shape cannot be easily determined without a complete numerical analysis. Hence, for the case of a perforated metal plate, or sheet, that had a sizeable number of large perforations the buckling coefficient was observed to decrease with an increase in size of the perforation in the metal plate. In a subsequent study, Sirkis and Lim [11] used an automated grid method to help analyze both displacements and strains developed in a perforated plate of an aluminum alloy when subject to loading. They observed and recorded plastic deformation to occur at locations immediately surrounding the perforation pattern. Chen [12] investigated the plastic deformation response of a metal sheet by employing an equivalent continuum approach for a perforated metal sheet. Results of their stress versus strain analysis was obtained by use of the finite element method coupled with actual experiments under condition of uniaxial tension in both the X direction and Y direction, and was found to be essentially isotropic. Upon being subject to plastic deformation, an observable amount of anisotropy was observed. Results for both the stresses and strains, under conditions of 'local' deformation, were found to be consistent upon comparison of the finite element analysis results with the experimental results.

Over the years, few other attempts have been made to characterize the mechanical behavior of perforated metal sheets by few independent research studies [13-17]. Garino and co-workers [18] discussed the results obtained from using the technique of finite element simulation and compared the results obtained from numerical analysis with experimental results for a cylindrical bar. They concluded from their results that use of the finite element technique in conjunction with large strain elastic-plastic models was an essential requirement for the purpose of simulating a simple tension test. With the aid of finite element simulation of a simple tension test, the large strains were computed and subsequently used for purpose of determining the displacements, strains and stresses experienced by both the nodal points and link elements in a perforated sheet of metal. Their results were also verified with results obtained from experimental tests. Norris and co-workers [19] performed finite element simulation for the purpose of calculating both the stress and strain at the time of fracture during elastic-plastic analysis. They found from their computation that both the stresses and strains had a maximum gradient at the center where fracture tended to occur while having a minimum value at the edges.

In the present study, an analytical model is designed and simulated for the purpose of determining displacements experienced at the joints arising from an intersection of the elements, or links, in a perforated metal plate, having a regular array of square perforations. The displacements obtained at the intersecting link elements forms a pattern of grid structures. For the case of both symmetric loading and asymmetric loading, the pattern of displacement occurring at the nodal points was determined and is graphically represented on a three-dimensional bar graph. This was done for different levels of the applied load and the resultant pattern of displacements obtained for the two chosen steels are compared.

2. THE MATERIALS CHOSEN

It is fairly well known from the principles of Materials Science that intrinsic microstructural features and

Table 1: Nominal Chemical Composition of the Two Hard Metals Chosen for Purpose of Analysis (In weight percent.) [From Reference 20]

Material	Fe	Cr	Mn	C	Si	Mo	S	P
4140	Balance	0.80-1.10	0.75-1.0	0.380-0.430	0.15-0.30	0.15-0.25	0.040	0.035
1018	Balance	-	0.6-0.9	0.14-0.20	-	-	0.040	0.050

Table 2: Uniaxial Tensile Properties of the Two Hard Metals Chosen for this Study [From Reference 20]

Materials Used	Density	Elastic Modulus		Tensile Strength		Yield Strength		Elongation in 50 mm (2 in)	Poisson's Ratio
		GPa	Ksi	MPa	Ksi	MPa	Ksi		
4140	7.85	205	29732.73	855	124	415	60.19	15	0.29
1018	7.87	205	29732.73	440	63.8	370	53.7	25	0.29

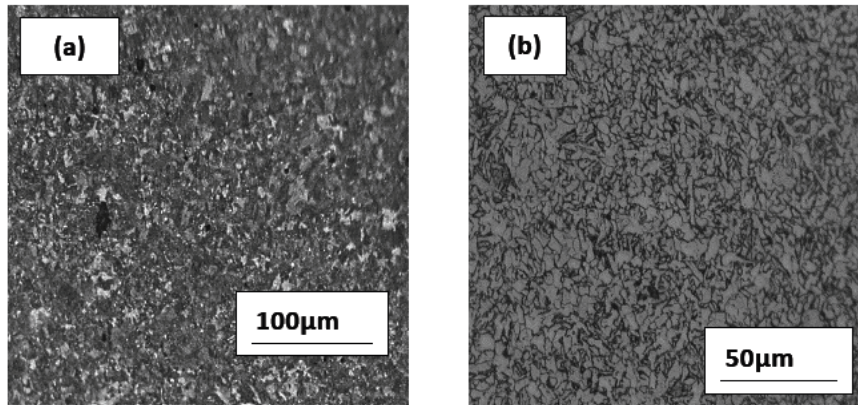


Figure 1: Optical micrographs showing microstructure of the two chosen steels: (a) Alloy steel 4140 with the two key micro-constituents: pearlite and ferrite. (b) Carbon steel 1018 with the two key micro-constituents: cementite and ferrite.

microstructural effects do play an important role in influencing the elastic - plastic behavior of a metal. The two metals chosen for this study were the following: (a) Carbon steel (i.e. AISI 1018) having a carbon content of 0.18 pct., and (b) Alloy steel (i.e., AISI 4140) having a carbon content of 0.40 pct. The nominal chemical composition of the two steels is provided in Table 1 [20]. The basic mechanical properties of the two chosen steels are summarized in Table 2 [21].

The alloy steel, commensurate with its high strength, revealed a microstructure comprising predominantly of dark regions, which is the pearlite

micro-constituent inter-dispersed randomly with pockets of “white” or “precipitate-free” region, namely the ferrite micro-constituent. Overall, the microstructure of this alloy steel in the as-provided condition was a combination of pearlite and ferrite (Figure 1a). The carbide particles, of varying size, were randomly distributed through the microstructure. The carbon steel, i.e., 1018 revealed a sizeable fraction of “white” regions, or ferrite micro-constituent, inter-dispersed with traces of the dark region, or cementite. In the white, or precipitate-free region, the grains were non-uniform in size and having a near needle-shape morphology (Figure 1b).

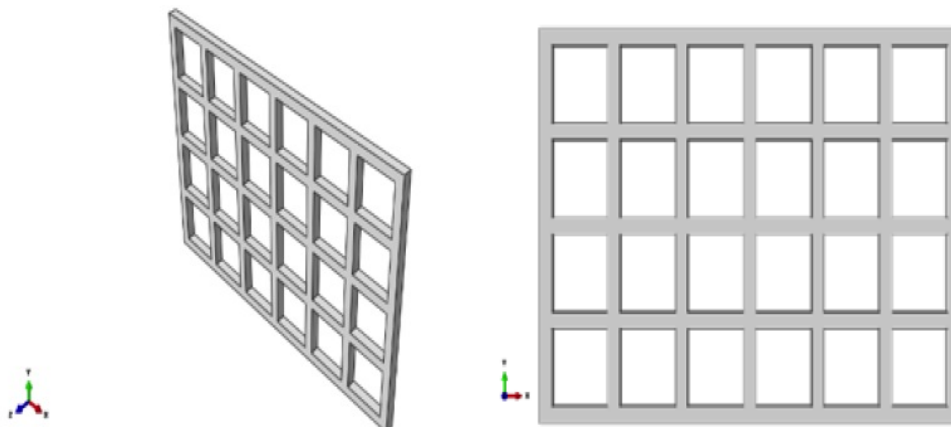


Figure 2: The perforated metal plate comprising of a network of thin links or thick link elements: (a) Three-Dimensional view, (b) Two-dimensional view of the metal plate.

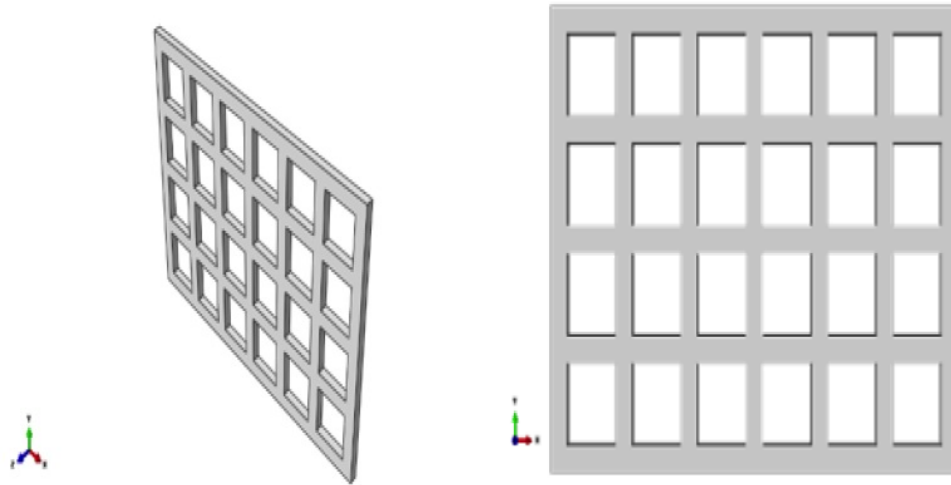


Figure 3: The perforated metal plate comprising of a network of thick links or thick link elements (a) Three-Dimensional view, (b) Top-dimensional view of the metal plate.

3. TEST SPECIMEN DESIGN / CONFIGURATION

A square perforation pattern for the two metals was chosen for purpose of analysis. The major idea for using a metal sheet having square-shape perforations is primarily because of the following: (i) its ability to be versatile, (ii) offer adequate strength, (iii) be functionally acceptable, while concurrently (iv) offering an overall acceptable visual appeal for use in products spanning a range of applications in the domain of engineering. The perforated metal sheet essentially resulted in a structure containing a network of numerous fine links as shown in Figure 2 and Figure 3. The linked metal structure has the ability to offer light weight, a high strength-to-weight ratio coupled with acceptable mechanical strength when compared with a solid piece of the same metal having identical thickness. A perforated sheet of the chosen metal comprises of numerous links that are assumed to be near-uniform in thickness.

Also, a perforated sheet of metal that is held together by a network of fine links does reveal differences in strength and mechanical response depending upon the direction of loading. For purpose of use in actual real-world applications both strength and stiffness properties of the perforated metal sheet are both important and essential. In fact, these two properties are important for purpose of analysis of the linked metal structure. In actual real-world situations involving practical technology-related application, loading often involves a mixture of bending and elongation.

The effective elastic constant and Poisson's ratio are normally for the plane stress condition and during

in-plane loading of the perforated metal sheet that is held together by numerous links. By using mechanical properties of the chosen metal, it is possible to determine the deflection and / or deformation experienced by the link elements in a perforated metal sheet for the following two conditions:

- (i) Any level of thickness, i.e., structure containing thick links versus structure containing thin links, and,
- (ii) Level of application of the load.

The presence of the square-shape perforations in a metal sheet eventually results in a structure that is held together by a network of fine links. The perforations made in the chosen solid metal sheet were square in shape and uniformly spaced through the metal sheet. The metal sheet now containing perforations and held together by a network of links was chosen for purpose of analysis for various values of the applied load, as a function of the yield load. Two possible variations of the chosen metal sheet were considered in this study, namely:

- (a) A structure containing a network of thin links or plane stress, and
- (b) A perforated metal sheet containing a network of thick links or plane strain.

The thinner structure is shown in Figure 4 (a), while the thicker structure is shown in Figure 4 (b). Dimensions of the perforated metal plate now containing, or held together, by links are summarized in Table 3. Dimensions of the perforations in the metal

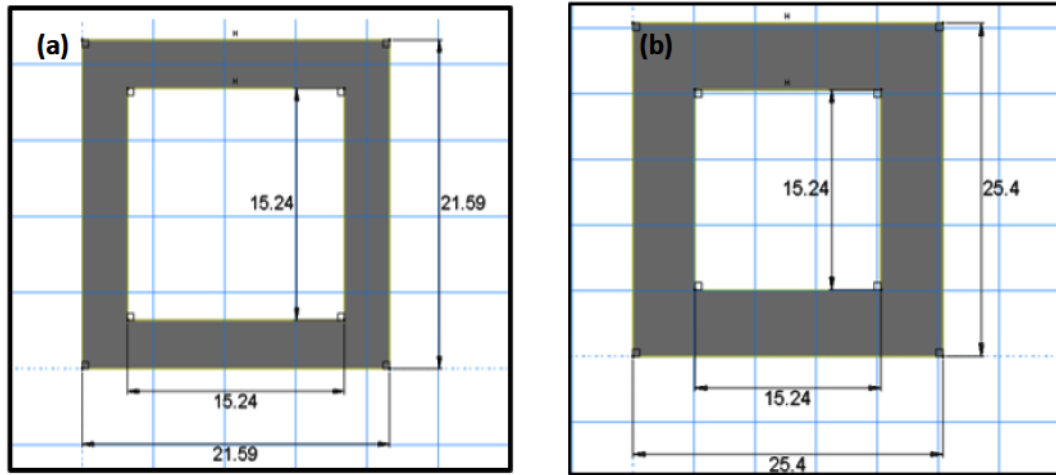


Figure 4: Dimensions of the links in the perforated metal plate. (a) Steel plate with thin links or link elements and (b) Steel plate with thick links or link elements.

Table 3: Dimensions of the Structure Containing Thin Links and Thick Links

	Thin Structure (mm)	Thick Structure (mm)
Length	113.67	127.00
Breadth	76.84	86.36
Thickness	3.18	3.18

Table 4: Dimensions of the Perforations Chosen to form the Linked Metal Structures used in this Study

Dimensions	Thin Structure (mm)	Thick Structure (mm)
External Length	21.59	25.40
External Breadth	21.59	25.40
Internal Length	15.24	15.24
Internal Breadth	15.24	15.24

sheet containing thin links and metal sheet containing a network of thick links are summarized in Table 4.

4. NUMERICAL PROCEDURE

4.1. Finite Element Formulation

The finite element analysis was carried out using general purpose finite element method. A static non-linear analysis was performed on the chosen metal plates having a number of square perforations. The equivalent stress was obtained for an isotropic material using the Von-Mises yield stress criterion. This failure criterion is often used for ductile metals, which tend to yield upon application of a load. For the situation of elastic-plastic analysis, when load is applied to a metal specimen, the stress is directly proportional to strain up

until the yield point is reached. The linear region, in which the stress (σ) is directly proportional to strain (ϵ) is governed by Hooke’s law. Once the applied stress crosses the upper yield point, or elastic limit, the region of non-linearity commences. This requires due consideration be given to an elastic-plastic analysis. When the applied stress exceeds the yield stress of the chosen metal, the metal plate of interest is no longer in the linear region of deformation.

The two chosen metals [carbon steel 1018 and alloy steel 4140] for purpose of performing finite element analysis with the objective of determining both the stress and displacements experienced by the link elements in a perforated metal plate or linked structure. Alloy steel 4140 had a yield strength [σ_{YS}] in pure tension of 476 MPa, and an ultimate tensile strength

$[\sigma_{UTS}]$ of 655 MPa. The modulus of elasticity of this steel is 205 MPa. The values of plastic strain were determined from the stress-versus strain curve with the aid of a web-plot digitizer. The strain values obtained from the stress versus strain curve comprises of both the elastic strain component and the plastic strain component.

4.2. Finite Element Simulation

This section utilizes the data for the chosen two steels used in this study from the Material's Data Handbook [20] for purpose of initiating simulation of the finite element method. The finite element code that was used for the purpose of conducting simulation under conditions of tensile loading was ABAQUS [Version 6.13.2]. The finite element method is useful primarily because it discretizes the chosen model into relatively small or fine elements, which are further divided into nodes for purpose of simplifying a complex model. This discretization into small elements plays an important role in numerical analysis, such that displacements experienced by an element provides a measure of both the extent and severity of distortion that occurs in shape of the element. The elastic-plastic analysis was performed using Newton Raphson iteration to determine both the stress and displacement with the aid of the finite element method. The finite element code ABAQUS Explicit was used in this analysis. Choice of the "explicit" solver arises from the fact that at equivalent plastic strain the Von-Mises yield criterion should be applicable for structures, such as: plates, having a uniform thickness. The "explicit" solution technique does offer a few advantages when compared to the "implicit" solution technique, which has been studied and results documented in the published literature by Proir [21]. Furthermore, for purpose of nonlinear analysis of the chosen steel it requires an incremental load or displacement step such that after every increment the results can be easily extracted due to a change in geometry of the starting structure as a consequence of the metal having either yielded or deformed into the domain of the non-linear region. This information is both essential and required for purpose of computing values of the stiffness matrix. Also, use of smaller elements, or finer increments, for purpose of nonlinear analysis does make the solution both accurate and precise but suffers from the drawback of being time consuming.

Two sheet metal structures, one having a network of thin links and the other having a network of thick

links, for each chosen steel [i.e., alloy steel 4140 and carbon steel C1018] were initially modelled and subsequently simulated using nonlinear analysis. The load levels chosen were (i) 10 pct. of the yield stress, (ii) 25 pct. of the yield stress, (iii) 50 pct. of the yield stress, (iv) 100 pct., of the yield stress, and (v) 102 pct. of the yield stress. Dimensions of the two chosen geometries, referred to henceforth as (a) structure containing a network of thin link elements, and (b) structure containing network of thick link elements, are summarized in Table 3 and Table 4.

A dependence of the elastic modulus (E) and Poisson's ratio (ν) on direction of loading is fairly well documented in the published literature. The presence and/or occurrence of 'local' stress concentration at the intersection of link elements does make the linked metal structure complex. This makes it both challenging and interesting for purpose of study, analysis, and evaluation. In considering the overall complexity of the model upon application of a load, it is essential to observe the behavior in the elastic range, since the presence of high 'local' stress concentration at the intersection of the link elements, can result in a non-uniform stress state to exist through the structure of a perforated metal plate, i.e., a structure containing a network of interconnected link elements. This makes mechanical testing not only complex but also challenging since loading of the metal plate that is held together by a network of links, or link elements, can result in premature failure by fracture of the links holding the metal plate together.

The criterion for yield at the different nodes in the perforated metal plate is expressed by the amount of load, as a fraction of the yield load of the metal, that is applied at the nodes of interest, which satisfies the criterion for loading in the direction of uniaxial tension. The displacement experienced by the nodes is recorded subsequent to the application of a load. Considering the centroid nodes in the structure to be at the intersection of two links, the displacements experienced by the nodes, or nodal points, are graphically represented on a three-dimensional bar graph. This bar graph provides a visual representation of the displacement experienced by a nodal point upon the application of a load. The bar graph can be used to compare with a similar hard material having near similar value for modulus of elasticity (E) and Poisons ratio (ν), while a change in composition does bring about an observable difference in the results obtained using the computational technique.

The two chosen metal plates were initially considered to be a plane stress problem, such that the approach for a layer was considered in ABAQUS. This helps in studying a complex model using the assumption of 2-D, which can be extended to a 3-D problem upon careful consideration of certain assumptions. In the 2-D assumption, the thickness of the plate, compared to its length, breadth, and width, was small or negligible. Herein, plane stress is the state of stress for which the normal stress $[\sigma_z]$ and shear stresses $[\sigma_{xz}$ and $\sigma_{yz}]$, are assumed to be negligible. Thus, an analysis of a thin plate of the chosen metal that was essentially loaded in the plane

of the metal plate was performed using the plane stress approximation. The load acting on both the X plane and Y plane are considered under conditions of plane stress.

The metal structure containing a network of links is as shown in Figure 5(a). The finite element model was created for the part of interest using the dimensions provided in Table 3 and an analysis was performed. For the two chosen cases, shown in Figure 2 and Figure 3, the non-linear large deformation formulation was used. The mesh that was chosen for use in the finite element analysis of the metal plate that contained

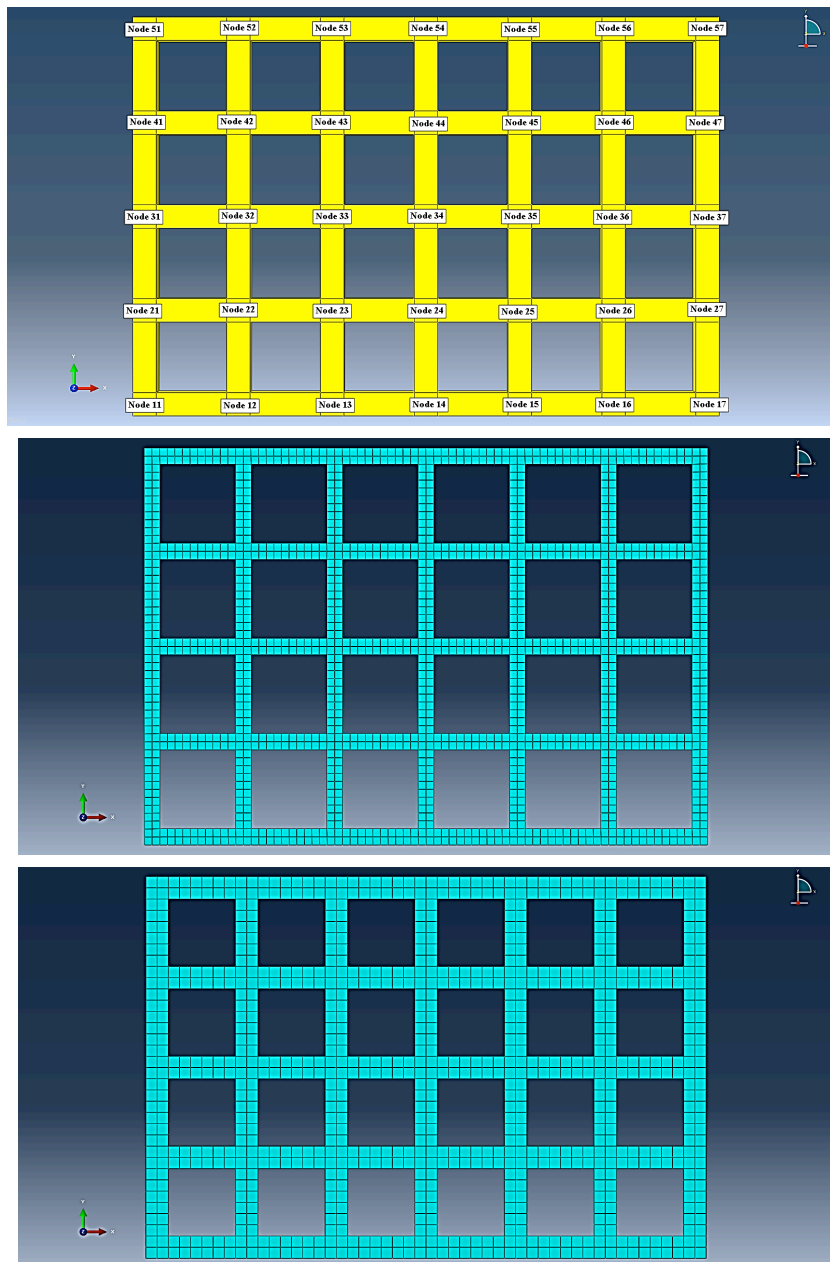


Figure 5 (a): A schematic of the metal structure containing a network of links with identification of the different nodes. **(b):** Size of mesh for a structure containing a network of thin links. **(c):** Size of mesh for a structure containing a network of thick links.

a network of thin links was a two-dimensional [2-D] mesh that had 1208 nodes and 325 elements. For the same metal plate that was held together by thicker links the mesh chosen contained 1000 nodes and 200 elements. For the two chosen cases, the calculations were performed using a two-dimensional, four node plane stress quadrilateral (CPS4) elements. Size of the element for a thin structure was 1.59mm *1.59 mm (Figure 5b) and size of the element for a thick structure the size was 2.54mm *2.54 mm (Figure 5c). To obtain a smooth curve for the variation of stress with strain, smaller increments were chosen and used. Re-meshing was avoided for purpose of analysis, since primary interest was in determining the displacement, occurring at the nodes or nodal points, with the objective understanding their magnitude and trend. For purpose of comparison of the two chosen steels, and the four different models [i.e., metal structure containing thin links and metal structure containing thick links for each chosen steel], the load applied to the linked metal structure was studied for two independent situations, herein referred to as: (i) Symmetric loading, and (ii) Asymmetric loading.

A two-dimensional [2-D] finite element analysis of the chosen mesh helps us to determine the displacements experienced by the nodes in the linked metal structure. In addition to 2-D modelling, calculations were performed for a full three-dimensional [3-D] representation of a perforated metal sheet that was held together by links using the eight node brick elements. A careful observation of the data resulting from numerical computation revealed the results provided by the three-dimensional [3-D] model did not significantly differ from those of the 2-D plane stress model in the domain of elastic deformation. Henceforth, all of the numerical results presented in this paper will be for the 2-D or the plane stress condition. The ultimate goal is to compute the results using the correct input parameters, to include the following: (i) properties of the chosen steels, (ii) dimensions of the structure, (iii) step time, (iv) magnitude of applied load used as function of the yield load of the chosen steel, and (v) boundary conditions. Upon performing the finite element analysis, we obtained fairly consistent results from our analysis. Prior to the initiation of numerical computation, it is essential to apply the boundary conditions carefully on the chosen model. To fix the chosen model in space for purpose of application of load we assumed one end of the linked metal structure to be fixed, while the other end of the linked metal structure, or perforated metal sheet, is subject to constraints in displacement.

The finite element analysis involved the following: (i) creating and meshing 2-D geometry for the square perforated steel plate, (ii) specifying suitable material properties of the chosen steel, (iii) applying the desired load, as a percentage of yield load of the chosen steel, and (iv) specifying the boundary condition. Essentially, the analysis was for the purpose of quantifying deformation experienced by both the nodes and link elements, which was modeled using ABAQUS software. The 2-D model was modeled using ABAQUS [version 6.13.2] for plane stress solid elements (CPS4), i.e., essentially a general purpose 4-Node linear brick element.

4.2.1. Properties of the Chosen Material

Mechanical properties of the two chosen steels are summarized in Table 2. The values of elastic modulus (E) and Poisson's ratio was chosen with respect to the steel plate chosen for purpose of numerical analysis [20]. For purpose of analysis of the chosen steel plate in the domain of plastic deformation the values of yield stress and corresponding plastic strain were specified depending on the chosen steel. In the region of non-linear deformation, the total strain comprises of the elastic strain component and the plastic strain component. The value of plastic strain was obtained using the relationship:

$$\epsilon_{total} = \epsilon_{elastic} + \epsilon_{plastic}$$

$$\epsilon_{plastic} = \epsilon_{total} + \sigma_{stress} / E$$

The values of plastic strain were obtained using a plot digitizer.

4.2.2. Boundary Conditions and Loading

Two types of boundary conditions were applied for purpose of simulating a simple tensile test. A boundary condition was applied to constrain rigid boundary rotation of the structure in space. This necessitated the need to constrain Node [1] and Node [2], using the CSYS global co-ordinate system in which displacements in both the X-direction (i.e., u_1) and Y-direction (i.e., u_2) were pinned. The Node [3, 1] and Node [4, 1] were constrained using the CSYS global co-ordinate system and their movement in the Y-axis was restricted. A point load was applied at the following two nodes, or nodal points, in the grid:

- (i) Node [2, 6], and Node [4, 2] for the case of Symmetric loading, and,

- (ii) Node [2, 6], and Node [4, 1] for the case of Asymmetric loading. The point load was applied at an angle of 45° to the horizontal. The load chosen for purpose of application was done in conformance with percentage of yield load for the perforated steel sheet containing thin links and the perforated steel sheet containing thicker links. The forces were resolved into components and applied at the two chosen nodes in the grid. For purpose of analysis, it is assumed that the load was distributed equally at the two chosen nodes, i.e., Node [2, 6], and Node [4, 1] at which it was applied.

4.2.3. The Mesh

In finite element analysis, it is desired to both create and use a mesh that has the least number of elements so as to minimize the time required for analysis while concurrently obtaining accurate results. The perforated metal sheet that is essentially held together by a fine network of links was portioned in a manner such that at the intersection of any two links, we get a four-4 node linear brick element. For purpose of analysis, a coarse mesh was chosen for each of the chosen steel structures. An element having a size of 1.59mm by 2.54mm was chosen for:

- (a) The perforated metal plate that was essentially held together by a network of thin link elements resulting in the formation of 1869 nodes, and
- (b) The metal plate held together by network of thick link elements resulting in the formation of 1292 nodes.

The sheet was taken to have one element through its thickness. The steel plate containing a network of thin link elements and steel plate containing a network of thick link elements were analyzed using the CPS4 element [a four-node bilinear plane stress quadrilateral shape element].

4.3. Static Analysis using ABAQUS

The perforated metal sheets of the two chosen steels were modelled using ABAQUS for Finite Element Analysis (FEA). Calculation of the load applied to the linked metal structure is obtained as a percentage of yield load of the chosen steel. For purpose of application of the load, two conditions, referred to as: (i) symmetric loading, and (ii) asymmetric loading, were chosen and studied.

- (i) Symmetric loading condition, the load was applied at two opposite ends of the perforated steel plate, i.e., at node point [2, 6] and node point [4, 2].
- (ii) Asymmetric condition, the load was applied at the following two nodal points, i.e., Node [2, 6], and Node [4, 1]. The situation of asymmetric loading was obtained by merely shifting the point of load application to an adjacent node. This does cause a change in the distribution of stresses, strains and displacement experienced by both the link elements and nodal points as a consequence of a change or shift in point of application of the load by one node thereby ensuring a shift from symmetric loading to asymmetric loading.

Five different levels of load were chosen for this study. The first four levels of load chosen and used were well within the elastic limit of the chosen perforated sheet metal, i.e., (i) 10 pct. σ_{YS} , (ii) 25 pct., σ_{YS} (iii) 50 pct. σ_{YS} and (iv) 100 pct. σ_{YS} of the yield load, while the fifth load was slightly above the yield load i.e. well into the plastic region of the stress versus strain curve. The amount or extent of load was used to study the distribution of stress, strain and resultant displacements experienced by the different links and nodal points of the linked metal structure.

The four simulation models that were designed for purpose of analysis of the square perforated metal

Table 5: Nodes Chosen for Application of Load for both Symmetric and Asymmetric Loading

Loading [pct. Of Yield Load]	Symmetric Loading for 1018 Carbon Steel (Thin and Thick Links)	Asymmetric Loading for 1018 Carbon Steel (Thin and Thick Links)	Symmetric Loading for 4140 Alloy Steel (Thin and Thick Links)	Asymmetric Loading for 4140 Alloy Steel (Thin and Thick Links)
10.0	[2, 6] and [4, 2]	[2, 6] and [4, 1]	[2, 6] and [4, 2]	[2, 6] and [4, 1]
25.0	[2, 6] and [4, 2]	[2, 6] and [4, 1]	[2, 6] and [4, 2]	[2, 6] and [4, 1]
50.0	[2, 6] and [4, 2]	[2, 6] and [4, 1]	[2, 6] and [4, 2]	[2, 6] and [4, 1]
100.0	[2, 6] and [4, 2]	[2, 6] and [4, 1]	[2, 6] and [4, 2]	[2, 6] and [4, 1]

plate under conditions of plane stress are the following, and detailed in Table 5.

- (i) The first model represents perforated alloy steel 4140 held together by thin links.
- (ii) The second model represents the perforated metal plate of carbon steel 1018 held together by thin link elements.
- (iii) The third model represents the perforated plate of alloy steel 4140 containing thick links.
- (iv) The fourth model represents the perforated plate of carbon steel 1018 containing thick link elements.

A coarse mesh was used around the square perforation for the metal structure containing thin links (Figure 5b) and for the metal structure containing thick links (Figure 5c).

5. RESULTS AND ANALYSIS

A 3D bar graph was used to plot the results and a pattern was observed after plotting the displacements experienced by the nodal points of the linked metal structure or perforated metal plate. The outputs were extracted for the five chosen levels of load that was applied to: (A) a linked metal structure containing a network of thin links, and (B) a linked metal structure containing a network of thick links. The 3-D bar graph provides a pattern for the displacement experienced by the nodal points and is compared with the pattern observed using electrical mesh topology. For the case of symmetric loading and with the requirement of mutually compatible load conditions at the common boundary of adjacent squares of the element, it was sufficient to consider a 45° segment and the boundary conditions were applied.

The primary focus is to determine the displacements occurring at the nodal points of the chosen linked metal structure. This will help establish the displacement pattern for the perforated metal plate that is held together by a network of link elements when subjected to loading in the tensile direction for the case of both symmetric loading and asymmetric loading. A pattern, or profile, was observed for the displacements by way of contours, and the numerical values were obtained using finite elements in synergism with numerical analysis. The pattern that was obtained is carefully analyzed by a comparison of the results obtained for the two chosen steel structures,

i.e., alloy steel 4140 and carbon steel 1018, for varying levels of applied load, using the finite element analysis. A 2-D approximation of the linked structure of the chosen steel plate was analyzed, assuming a plane stress condition to prevail, using the finite element stress analysis. For both symmetric loading and asymmetric loading, the contours obtained were quite similar to the results obtained for the 3-D model.

5.1. A Comparison between Thin Structures of Alloy Steel 4140 and Carbon Steel 1018

5.1.1. Symmetric Loading of Alloy Steel 4140 and Carbon Steel 1018

The linked metal structure of alloy steel 4140 was found to deform from its original shape and the following observations, with specific reference to displacements experienced by both the nodes and links, are recorded for the five chosen load levels, as a function of yield stress of the chosen metal. A few of the key observations are highlighted with respect to the method chosen.

The stresses were randomly distributed through the entire structure of alloy steel 4140 containing a network of thin links, which can be observed by examining Figure 6. The structure does contain few points of high local stress concentration arising due to the presence of square shaped perforations. Hence, under the influence of an external mechanical stimulus, or load, the region both at and near the square perforation experiences a higher level of stress, whereas the region between the links experiences minimal value of stress. The magnitude of stress both at and around the nodes is noticeably high in comparison with the stress occurring at the middle of the links. Profile of the contours of the von-Mises stress for this steel containing a network of thin links is shown for the case of applied load being 100 pct. of the yield load in Figure 6(a) and for applied load being 102 pct. of the yield load in Figure 6(b).

For the linked metal structure of alloy steel containing a network of thin links, the maximum displacement was found to occur at the nodal points situated towards the upper half of the perforated metal plate. The magnitude of displacement at the middle of the metal structure containing a network of thin links was noticeably less. A profile of the displacements experienced by the different nodes of the linked metal structure of alloy steel 4140 containing a network of thin links, when subject to symmetric loading, is shown in Figure 7 for the chosen values of the applied load, as

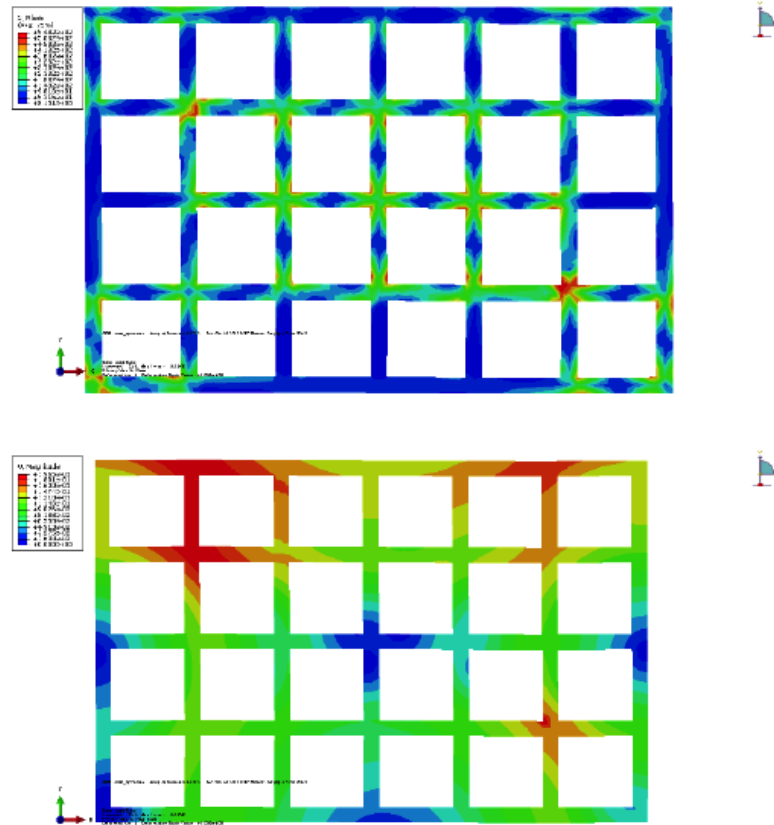


Figure 6(a): Profile showing contours of the Von Mises stress for alloy steel 4140 that was subjected to symmetric loading at Node (2,6) and Node (4,2) for the metal structure containing a network of thin links at yield stress (σ_{YS}) of the material. **(b)** A contour profile showing the magnitude of displacements experienced by linked structure of alloy steel 4140, containing a network of thin links, when subjected to symmetric loading at 102 pct. of the yield stress.

percentages of the yield stress. The upper region of the linked structure experiences more deformation on Row 4 and Row 5, when compared to the lower region i.e. Row 2 and Row 1. The pattern upon close observation reveals a minimal effect on the centroidal node.

The three dimensional bar graph shown in Figure 7 reveal the pattern of displacement experienced by the centroid nodes in the metal structure of alloy steel 4140 containing a network of thin links. The values of displacement were obtained from results of the finite element analysis that was performed on a laboratory-scale computer. The outputs were extracted in the visualization module of ABAQUS/CAE-6.13-2. The point of attention is the centroid, which is identified by its location at the intersection of two links. Deformation, or displacement, experienced by the linked metal structure initiates once a higher stress occurs at the center of the links in a given mesh. The area of interest is the region contained within the linked metal structure comprising a network of thin links, which upon being subject to loading the magnitude of displacement experienced by the centroid nodes are represented by

a 3D bar graph. The displacements were recorded for five levels of load applied as a function of yield stress of the chosen metal, i.e., 10 pct. σ_{YS} , 25 pct., 50 pct. σ_{YS} , 100 pct. σ_{YS} and 102 pct. σ_{YS} . The percentages of the yield stress are chosen with respect to the steel chosen for the analysis. Below the yield stress the alloy steel structure containing a network of thin links upon being subject to symmetric loading, the maximum deflection was observed to occur at the point of application of load, i.e. Node [2, 6] and Node [4, 2], while Node [3, 4] experienced minimal amount of deformation, since the structure is assumed to be symmetric along both the X axis and Y axis. Hence, we did observe a minimal influence on the centroidal node of the structure containing a network of thin links.

The linked metal structure of carbon steel 1018 containing a network of thin links as shown in Figure 5-b. The Von Mises stress in carbon steel 1018 containing a network of thin links is relatively high when compared one-on-one with alloy steel 4140 at the two chosen load levels corresponding to: (i) 100 pct. of yield stress [σ_{YS}] (Figure 8a), and (ii) 102 pct. Of the

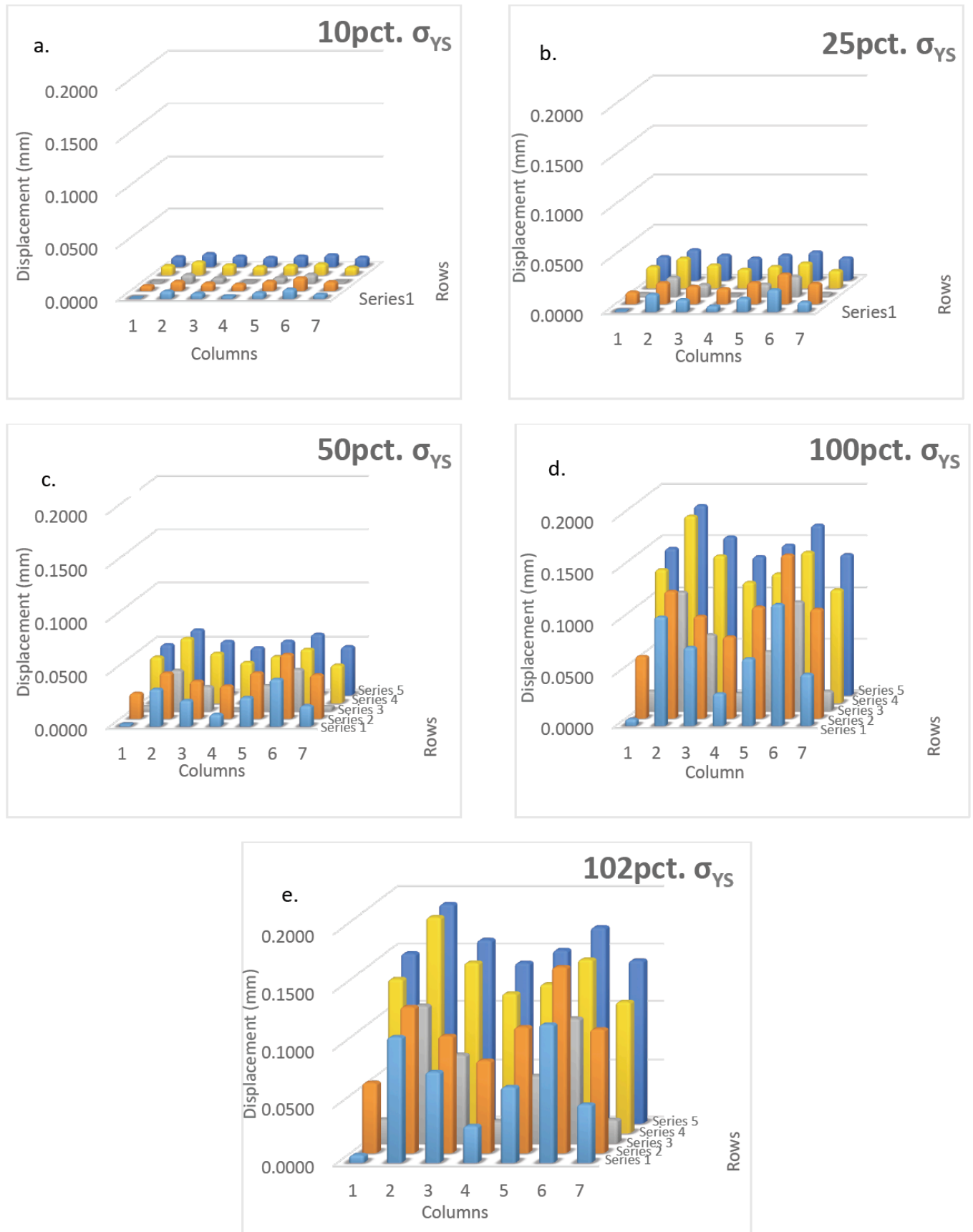


Figure 7: Profile showing the displacement experienced by the different nodes of the “thin” linked structure of alloy steel 4140 upon being subject to symmetric loading, applied at Node (2, 6) and Node (4, 2). (a) 10 pct. of yield stress. (b) 25 pct. of yield stress. (c) 50 pct. of yield stress. (d) 100 pct. of yield stress. (e) 102 pct. of yield stress.

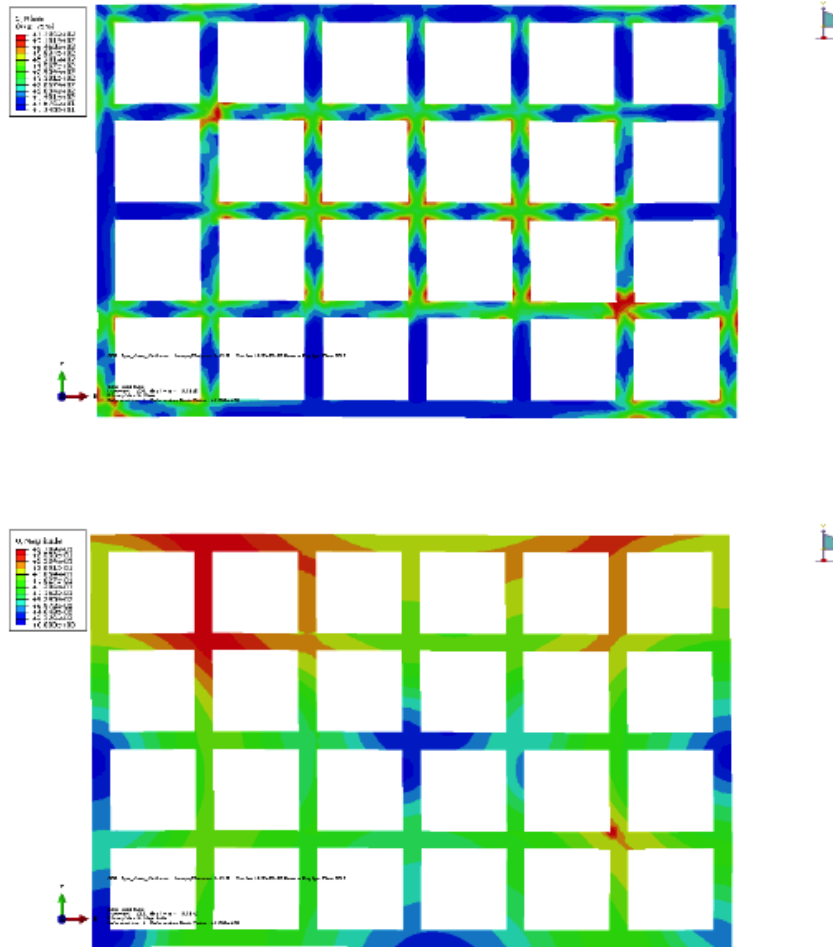


Figure 8(a): Profile showing the contours of the Von Mises stress for carbon steel 1018 that was subjected to symmetric loading at Node (2, 6) and Node (4, 2) for the structure containing a network of thin links at a load equal to yield stress of the material. **(b)** A contour profile showing the magnitude of displacements experienced by linked structure of carbon steel 1018, containing a network of thin links, when subjected to symmetric loading, 102 pct. of the yield stress.

yield stress (Figure 8b). This is based on an observation of the contours. In Figure 8(a) and Figure 8(b) reveal a similar contour, which exemplifies the occurrence of stress concentration to occur both at and immediately adjacent to an intersection of two links. The Von Mises stress and resultant plastic strain was found to be noticeably more in carbon steel 1018 when compared one-to-one with alloy steel 4140. This is rationalized on the basis of strength of the two chosen steels. The lower strength and resultant higher ductility of carbon steel makes it receptive to experience deformation by way of increased displacement of both the links and nodes upon loading. The deformation was evident from the values recorded for (i) displacement of the links, or link elements, and (ii) displacement experienced by the nodes.

Upon examination of the results obtained from numerical analysis, we observe a difference in values

obtained at the centroidal nodes, which brings to light the significance of results obtained using finite element analysis (FEA). To facilitate ease in understanding of the displacements, all the nodal points are shown through three dimensional bar graphs to provide an overview of the pattern obtained upon subjecting the structure, containing a network of thin links, to loading (Figure 9). From the bar graphs, we observe a much higher displacement to occur in carbon steel 1018 when compared one to one with alloy steel 4140.

5.1.2. Asymmetric Loading of Alloy Steel 4140 and Carbon Steel 1018

For the case of asymmetric loading, i.e. when the point of application of load is changed and a similar analysis is performed, we observe the displacement pattern does not change appreciably. The magnitude of displacement is fairly high and observable up to the nodes situated on Row 4. However, the magnitude of

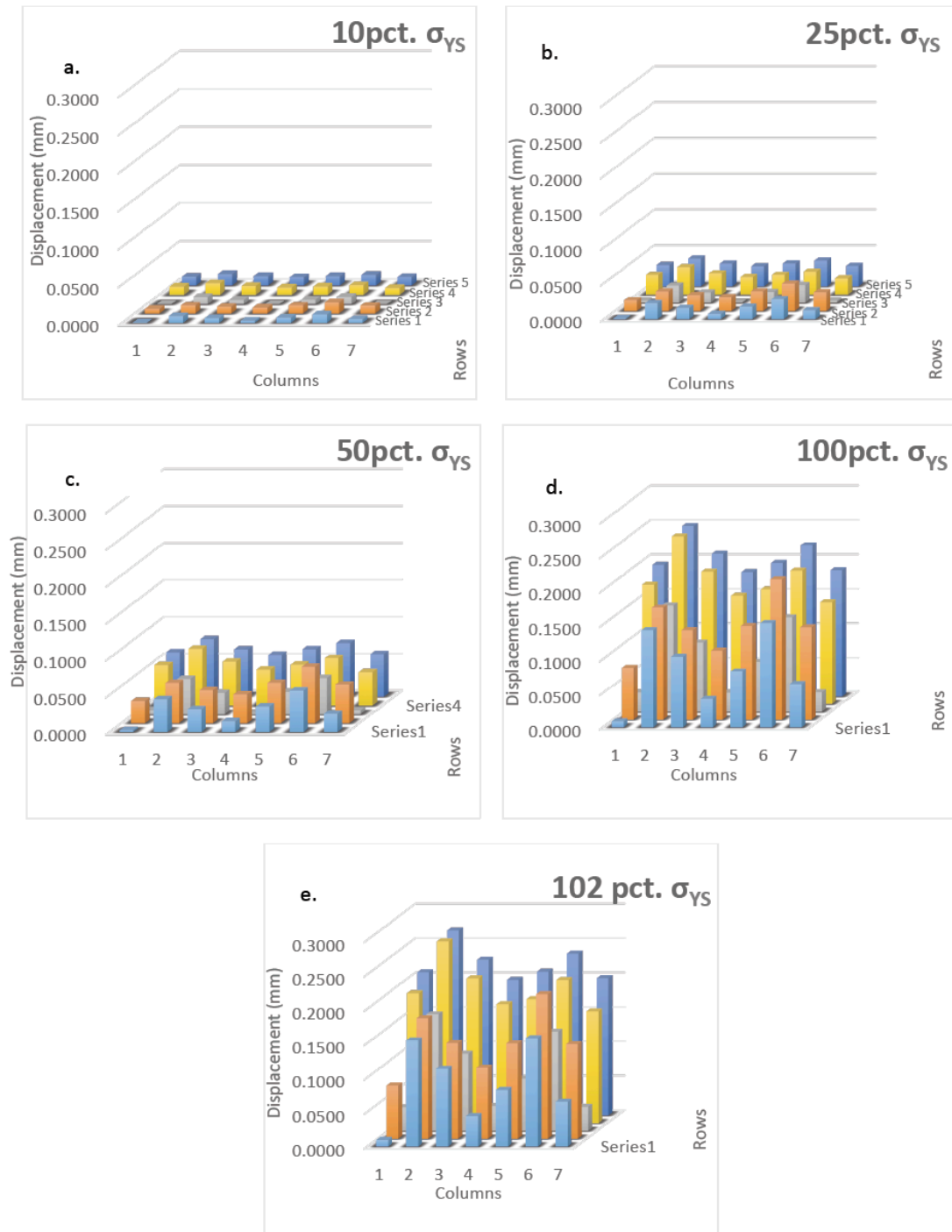


Figure 9: Profile showing the displacement experienced by the different nodes of the linked structure of carbon steel 1018, containing a network of thin links, when subjected to symmetric loading, applied at Node (2, 6) and Node (4, 2). (a) 10 pct. of yield stress. (b) 25 pct. of yield stress. (c) 50 pct. of yield stress. (d) 100 pct. of yield stress. (e) 102 pct. of yield stress.

displacement experienced by nodes located on Row 5 decreases, which is the opposite of what was observed for the case of symmetric loading. Also, an overall pattern of displacement recorded for the case of asymmetric loading was quite similar to the pattern observed for the case of symmetric loading. This is an interesting observation for the two chosen steels (i.e., alloy steel 4140 and carbon steel 1018), and the

pattern obtained takes a near “S”-shape when the values are plotted and represented graphically.

Upon application of an asymmetric load to alloy steel 4140 containing a network of thin links at the chosen load levels of 10 pct. σ_{YS} , 25 pct. σ_{YS} , 50 pct. σ_{YS} , 100 pct. σ_{YS} , and 102 pct. σ_{YS} , the maximum displacement was evident at the nodal points, or

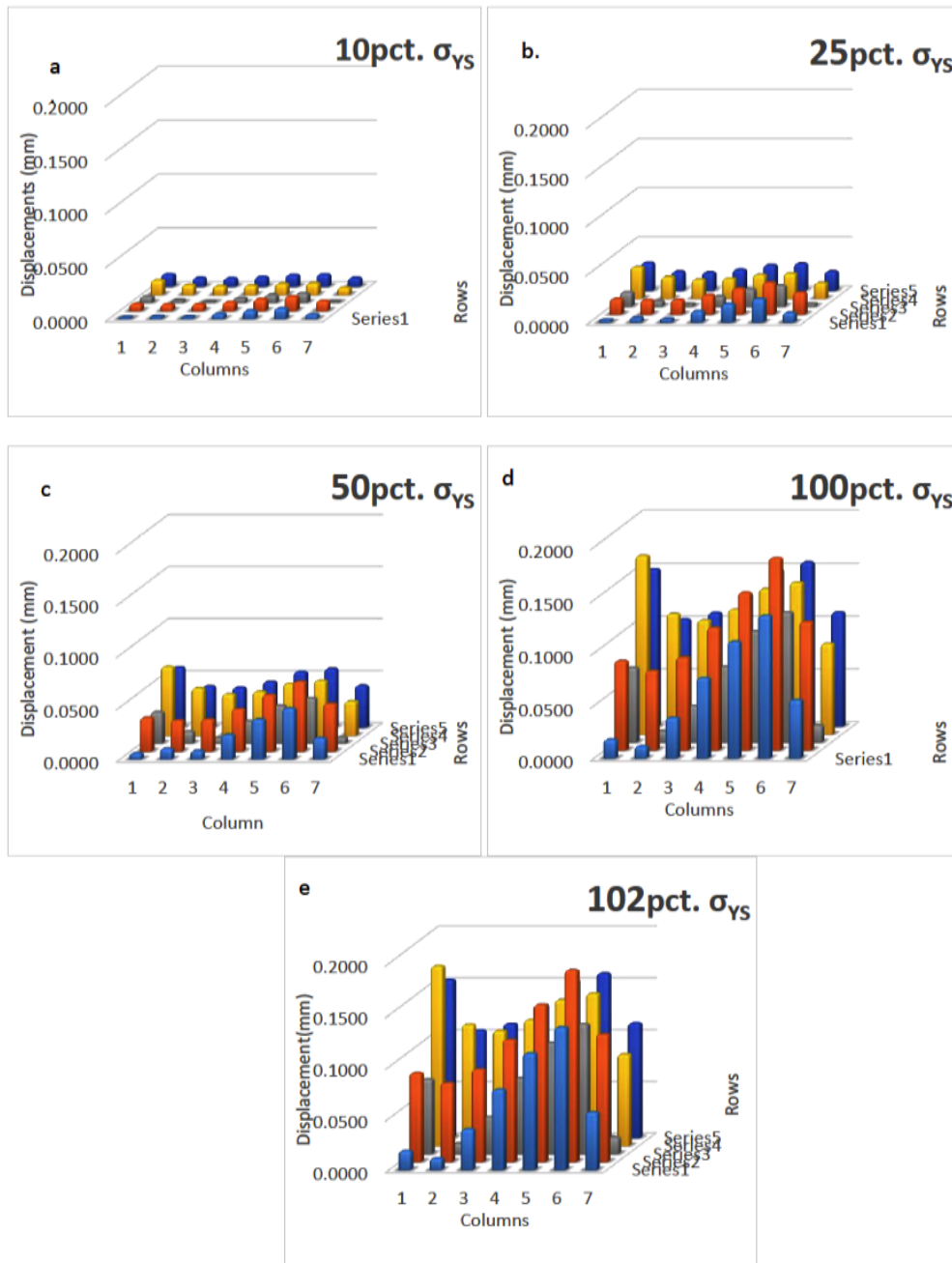


Figure 10: Profile showing the displacement experienced by the different nodes of the linked structure of alloy steel 4140, containing a network of thin links, when subjected to asymmetric loading, applied at Node (2,6) and Node (4,1). (a) 10 pct. of yield stress. (b) 25 pct. of yield stress. (c) 50 pct. of yield stress. (d) 100 pct. of yield stress. (e) 102 pct. of yield stress.

nodes, located towards upper half of the perforated metal plate (Figure 10). The displacement experienced by the different links, or link elements, in alloy steel 4140 were found to be quite similar when compared one-on-one with the displacements experienced by the network of thin links, or link elements, in carbon steel 1018 (Figure 11). Also, the displacement pattern when represented graphically on a 3-D bar graph reveals a kind of symmetry between the two chosen steels upon

application of a load. The magnitude of displacement experienced by the different links in the structure of the two chosen steels reveal a near-similar behavior when compared one-on-one with each other. The pattern represents low displacements occurring at the nodes on approximately 30 percent of the loaded metal plate while maximum displacement was observed to be occurring at those nodes that were located towards the upper half of the plate.

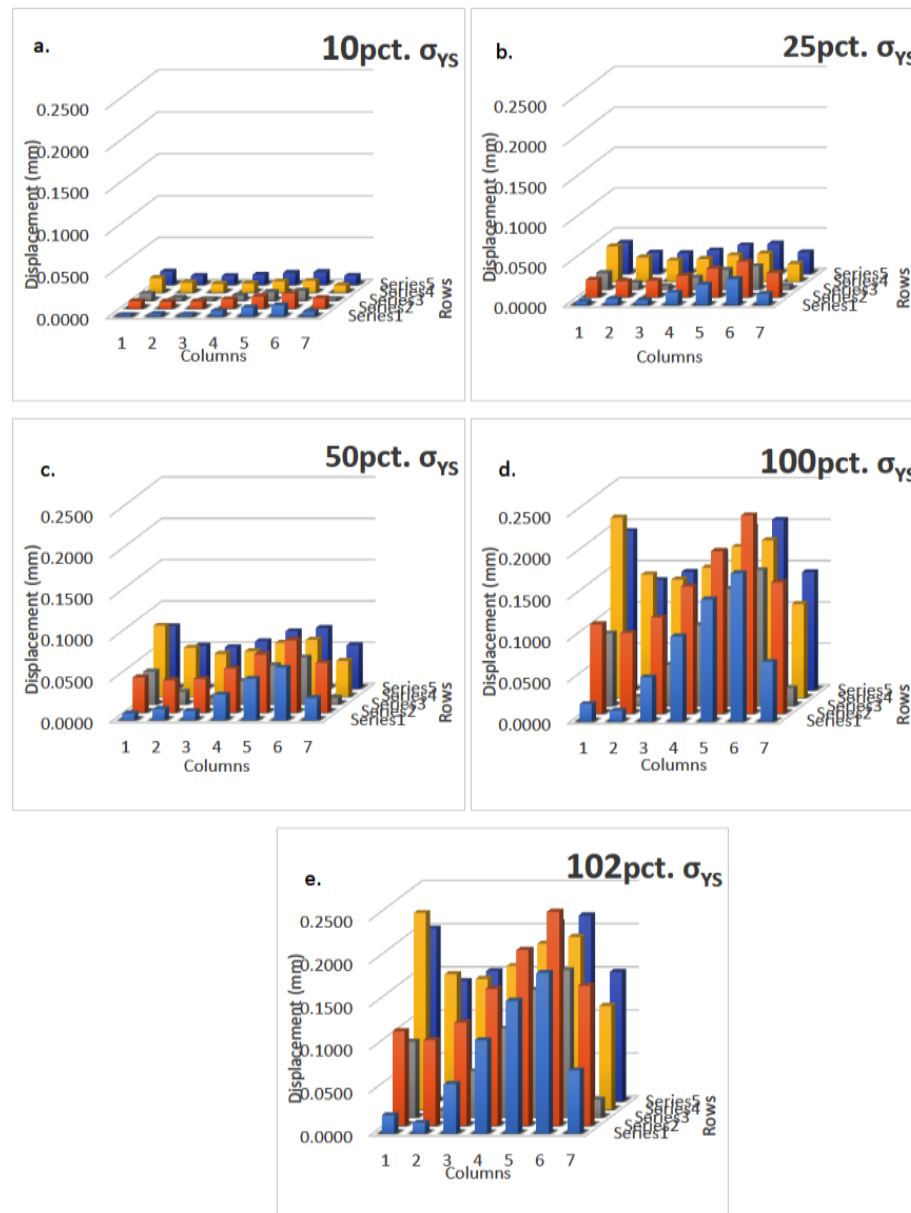


Figure 11: Profile showing the displacement experienced by the different nodes of the linked structure of carbon steel 1018, containing a network of thin links, when subjected to asymmetric loading, applied at Node (2,6) and Node (4,1). (a) 10 pct. of yield stress. (b) 25 pct. of yield stress. (c) 50 pct. of yield stress. (d) 100 pct. of yield stress. (e) 102 pct. of yield stress.

It is observed that when the loading is asymmetric, and at the two chosen values of 100 pct. the yield stress (Figure 12a) and 102 pct. the yield stress (Figure 12b), the maximum stress was observed to occur at the upper nodes of the steel metal structure. Overall, the nodes in carbon steel 1018 (Figure 13) provide a higher value of stress on the linked metal structure when compared one-to-one with the nodes in alloy steel 4140. This is a key factor that governs, or dictates, the viability of selecting this material for purpose of machining and use in products requiring extensive machining. The contours also provide a globally ductile behavior for carbon steel 1018 when compared one-on-one with alloy steel 4140.

Results obtained from analysis does reveal a noticeable difference in the values of displacement experienced by the centroidal nodes, which reiterates both the accuracy and importance of the results obtained using finite element analysis. To provide a better appreciation, all of the nodal points detailed in Figure 5(a) are shown in the three dimensional bar graphs to facilitate an understanding of the displacement pattern obtained when the structure containing a network of thin links is subject to loading. From the bar graphs we do observe noticeably higher value of displacement experienced by the nodes of linked metal structure of carbon steel 1018 when

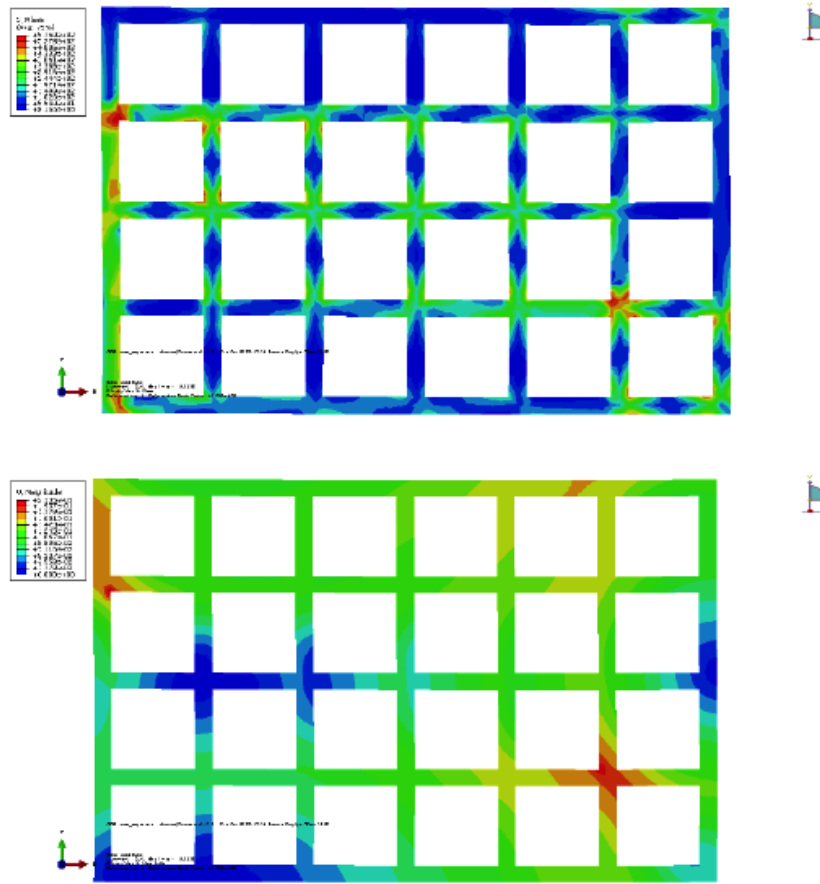


Figure 12(a): Profile showing the contours of the von Mises stress for alloy steel 4140 that was subjected to asymmetric loading at Node (2, 6) and Node (4, 1) for the structure containing a network of thin links and at load corresponding to yield stress of the metal. **(b)** A contour profile showing the magnitude of displacements experienced by linked structure of alloy steel 4140, containing a network of thin links, when subjected to asymmetric loading, at 102 pct. of the yield stress.

compared one-on-one with the nodes in linked metal structure of alloy steel 4140.

From Figure 6 to Figure 13, it is clear that when the structure containing a network of thin links is subjected to both symmetric loading and asymmetric loading, the center of the linked metal structure experiences minimal amount of deformation. However, when the loading is offset to an adjacent node, i.e., in essence asymmetric loading, the least deformation is found to occur at the centroidal node, i.e., Node [3, 2], which is an interesting observation. From the results obtained it is clear that when the loading is offset to another point, the overall contour of deformation experienced by both the nodes and links does reveal an observable change. For alloy steel 4140 (Figure 10), the lower node [2, 6] experiences a higher amount of deformation when compared to carbon steel 1018 (shown in Figure 11). This is evident from the bar graphs depicting the displacement pattern. Yielding of the metal structure containing a network of links initiates at Node [4, 1] for

the case of asymmetric loading of both carbon steel 1018 and alloy steel 4140. The displacements were observed to be gradually more towards the lower right half of the linked metal structure. The displacements are linearly increasing towards the right half of the chosen perforated metal plate and rather irregularly distributed towards the left half of the perforated metal structure.

5.2. A Comparison between Thick Link Structures of Alloy Steel 4140 and Carbon Steel 1018

5.2.1. Symmetric Loading Alloy Steel 4140 and Carbon Steel 1018

The 4140 alloy steel link structure initiated deforming from its original shape and the following observations, with specific reference to displacement, are recorded for the five chosen loading conditions, as fractions of the yield stress. The yield stress was obtained from the stress versus strain curve that generated by use of tensile test simulation performed

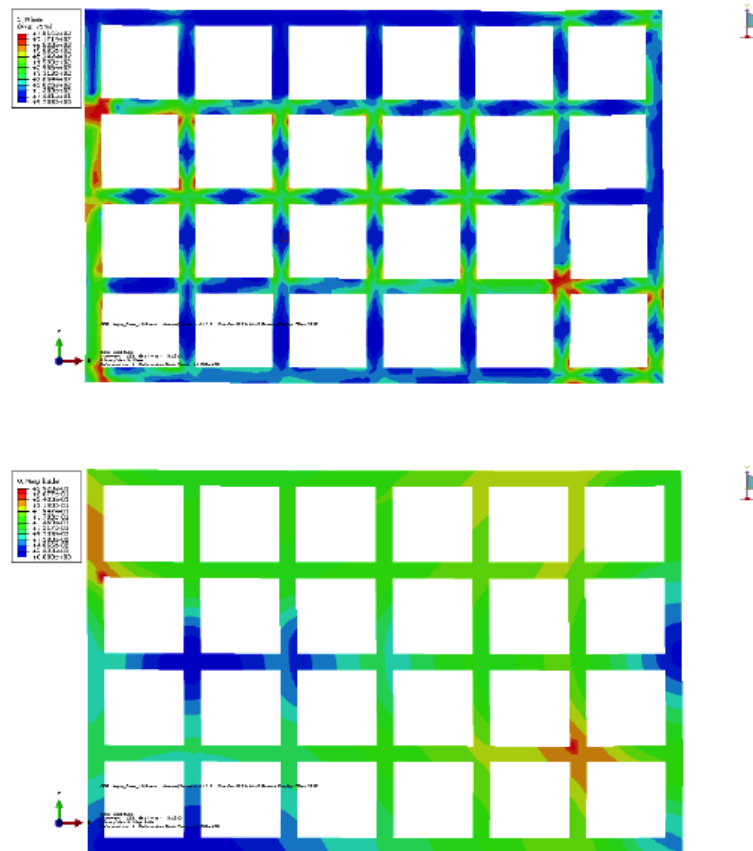


Figure 13(a): Profile showing the contours of the Von Mises stress for carbon steel 1018 that was subjected to asymmetric loading at Node (2, 6) and Node (4, 1) for the structure containing a network of thin links at a load corresponding to yield stress of the metal. **(b)** A contour profile showing the magnitude of displacements experienced by linked structure of carbon steel 1018, containing a network of thin links, when subjected to symmetric loading at 102 pct. of the yield stress.

on the structure containing a network of thick links. Upon symmetric loading in tension of alloy steel 4140 containing a network of thick links, the reaction forces were noticeably more towards the lower end, i.e. node [2, 6], resulting in a higher magnitude of the Von Mises stress in this region culminating in the early initiation of yielding for applied load corresponding to 100 pct. yield stress (Figure 14a) and for applied load corresponding to 102 pct. of the yield stress (Figure 14b). The contour of stress concentration occurring at the nodes, obtained at the intersection of four links, was noticeably high and observably minimal towards the center of the link. The trend shown by the displacement provides a completely different contour, when compared with the stress contour at an identical value of the applied load.

Upon application of load to the linked metal structure of alloy steel 4140 containing a network of thick links, the maximum displacement was observed to occur at the intersecting nodes situated both at and near the upper regime of the perforated metal plate. The magnitude of displacement experienced by the

different links in the thick linked structure of alloy steel 4140 shown in Figure 15, was found to be noticeably low when compared one-on-one with the same steel structure containing a network of thin links.

Also, the pattern of displacement when plotted on a 3D bar graph reveals a symmetry to exist between the two chosen steels, upon being subject to loading at the five chosen values of load. While the values of displacement are different they do show a similar behavior when compared one-on-one with respect to each other. At the upper left end of the perforated metal plate the displacement experienced by both the links and nodes was relatively low. This can be ascribed to the fact that at this location the actual effect of loading is reduced. Further, the load was applied equally at the two chosen nodes of the linked metal structure and the displacement experienced by the nodes was noticeably high at the upper half of the metal structure, when compared to the lower half of the same structure for the five chosen levels of applied load.

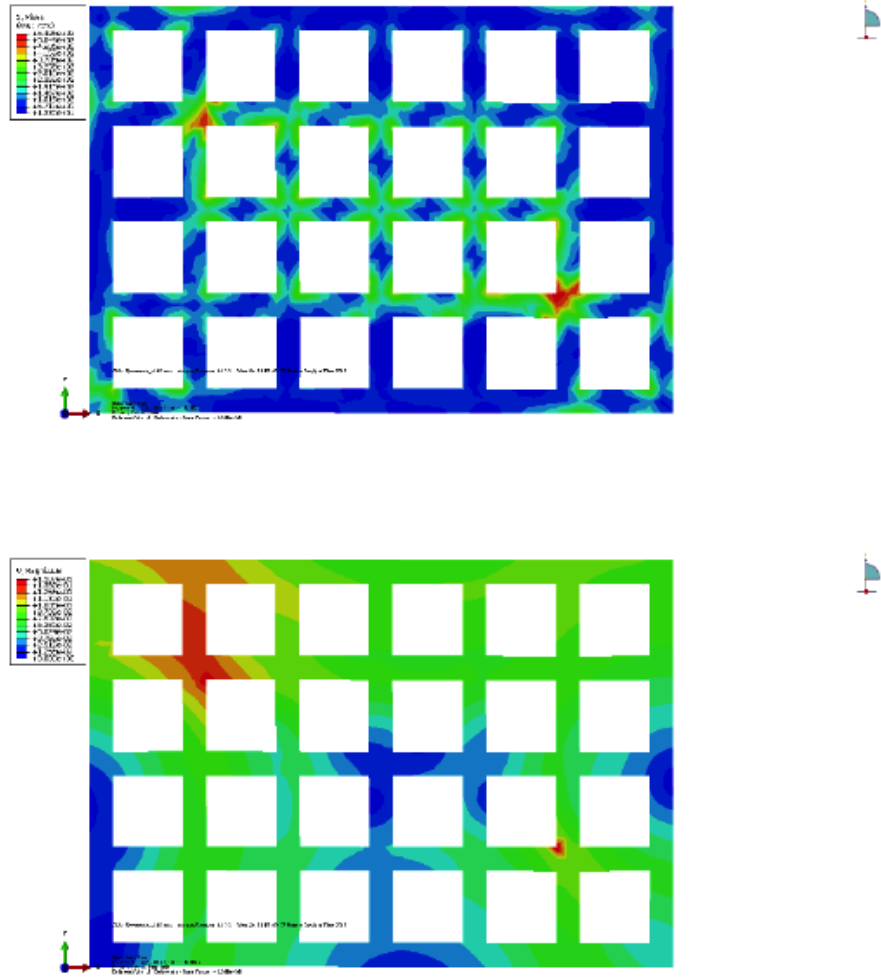


Figure 14(a): Profile showing the contours of the Von Mises stress for alloy steel 4140 that was subjected to symmetric loading for Node (2, 6) and Node (4, 2) of the structure containing a network of thick links at a load equal to the yield stress of the metal. **(b)** A contour profile showing the magnitude of displacements experienced by “thick” linked structure of alloy steel 4140 when subjected to symmetric loading, 102 pct. of the yield stress.

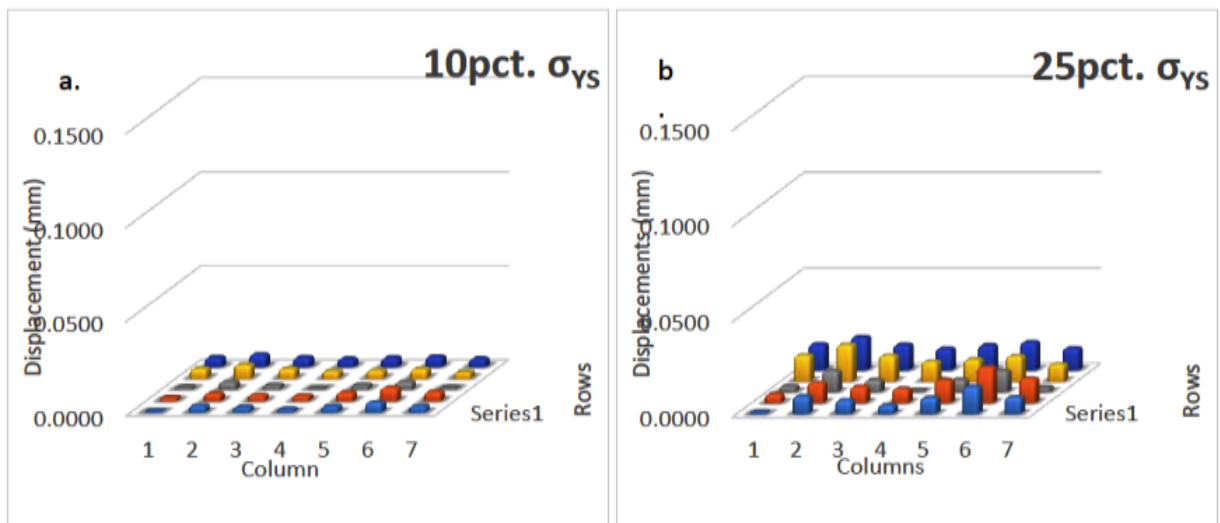


Figure 15 continued...

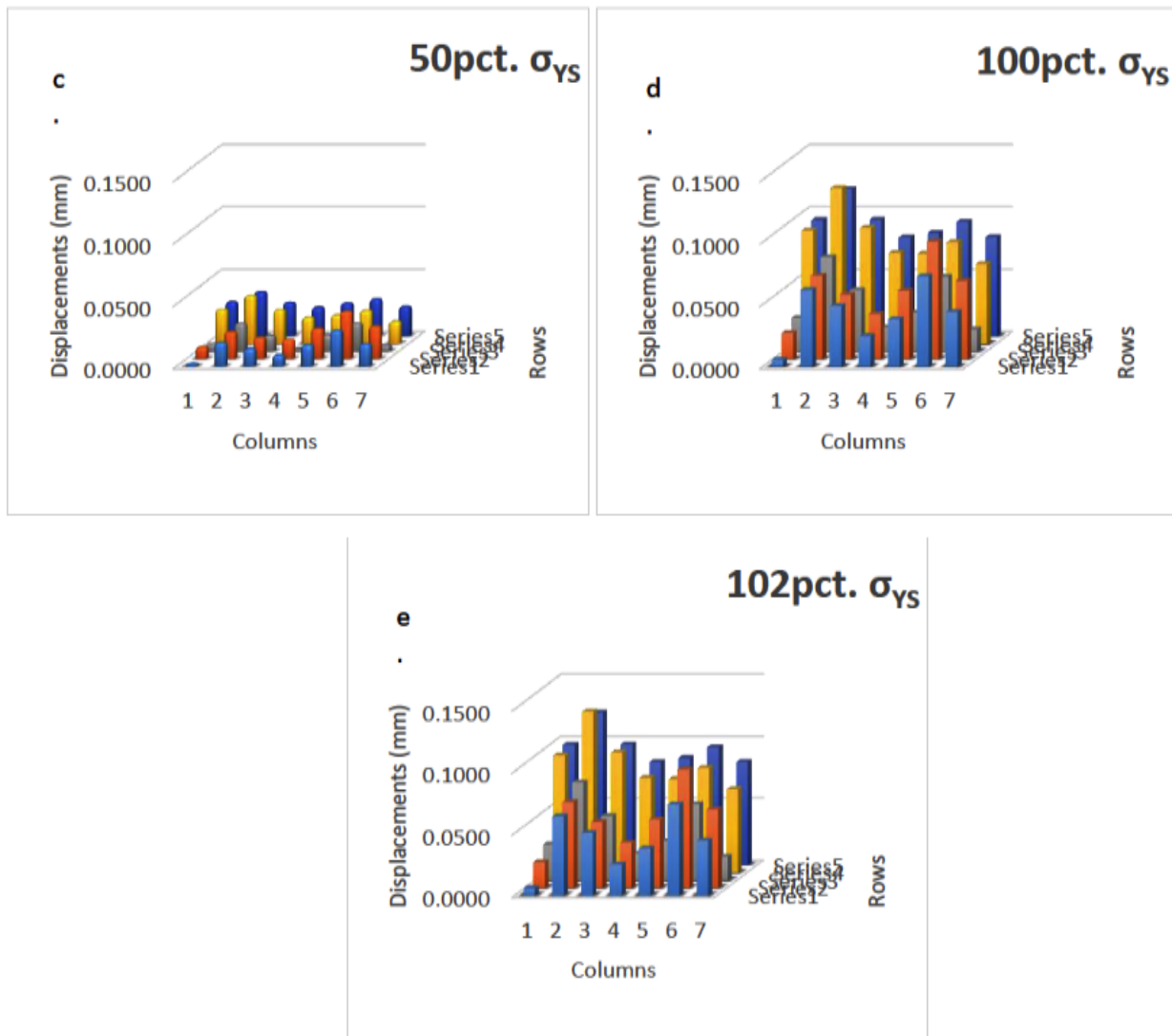


Figure 15: Profile showing the displacement experienced by the different nodes of the “thick” linked structure of alloy steel 4140 when subjected to symmetric loading, applied at Node (2, 6) and Node (4, 2). (a) 10 pct. of yield stress. (b) 25 pct. of yield stress. (c) 50 pct. of yield stress. (d) 100 pct. of yield stress. (e) 102 pct. of yield stress.

For carbon steel 1018, the structure containing thick links when subjected to loading, i.e., Node [2, 6], high values of the “local” stress initiate at the lower nodes of the linked structure due to which yielding is favored to initiate in this region. At applied load levels corresponding to 100 pct. of yield stress (Figure 16a) and load corresponding to 102 pct. of yield stress (Figure 16b), the upper half the linked metal structure experienced noticeably lower stresses when compared to rest of the metal structure. The displacements experienced by the nodes, were plotted on a 3D bar graph. The displacements experienced by the nodes in carbon steel 1018 were observably higher towards the right half of the metal plate and gradually decreased

towards the left side of the linked metal structure. The deformation, or displacement, experienced by the nodal points provide an insight of the nodes in carbon steel 1018 experiencing a higher value of deformation when compared one-on-one with the nodes in alloy steel 4140. This can be attributed to the higher strength of the chosen alloy steel 4140 and resultant lower ductility when compared to carbon steel 1018. A similarity between the linked structures of the two chosen steels is that the upper regions near the point of application of load experiences a higher level of deformation of the nodes, which is observed from the pattern shown in the bar graphs for the two chosen steels.

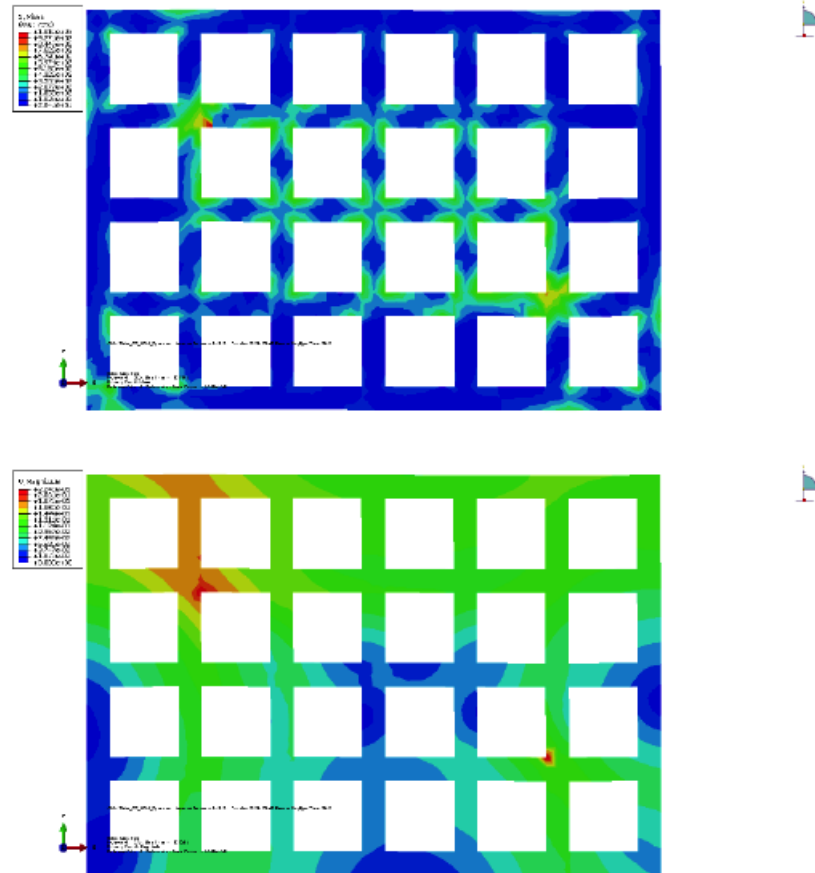


Figure 16(a): Profile showing the contours of the Von Mises stress for carbon steel 1018 that was subjected to symmetric loading for node (2,6) and node (4,2) of the thick linked structure at applied load corresponding to the yield load. **(b)** A contour profile showing the magnitude of displacements experienced by “thick” linked structure of carbon steel 1018 when subjected to symmetric loading at applied load corresponding to 102 pct. of the yield load.

5.2.2. Asymmetric Loading: Alloy Steel 4140 and Carbon Steel 1018

For alloy steel 4140 and asymmetric nature of loading, i.e. when application of the load is changed to an adjacent nodal point, we observe the contour pattern to change appreciably at the point of application of the tensile load. The upper region, i.e., the region near node [4, 1] experiences a higher level of the Von Mises stress, whereas the area towards the lower right half of the perforated metal plate reveals a similar profile, when compared one-on-one with symmetric loading. The stresses are noticeably more at the intersection of four links, or link elements, i.e. at the internal nodes, and comparatively lower in value both at and near the outer region of the metal structure. The stress profile for applied load level corresponding to 100 pct. of yield load is shown in Figure 18(a), and for an applied load level corresponding to 102 pct. of yield load is shown in Figure 18(b). The magnitude of displacement experienced by the nodes was noticeably more for those nodes situated in Row 4. The

magnitude of displacement decreases for the nodes on Row 5, which is vice versa of the observation that was made for the case of symmetric loading. Thus, for the two chosen steels, and ‘S’ shaped pattern for the displacement was observed when the data is represented on a bar graph.

Upon application of an asymmetric load to alloy steel 4140 containing a network of thick links, the maximum displacement at the five chosen load levels occurs at the intersecting nodes located towards the upper half of the perforated metal plate. Details of which by way of graphical presentation can be found elsewhere [23]. It is interesting to note that the lower half of the perforated metal plate, or linked metal structure, does not experience appreciable deformation when compared to the link elements and nodal points located towards upper half of the plate. Upon application of a load, the displacement contour reveals maximum deformation to occur in the region near Node [4, 1] and the surrounding links. Upon increasing the load, the minimal deformation experienced by Node

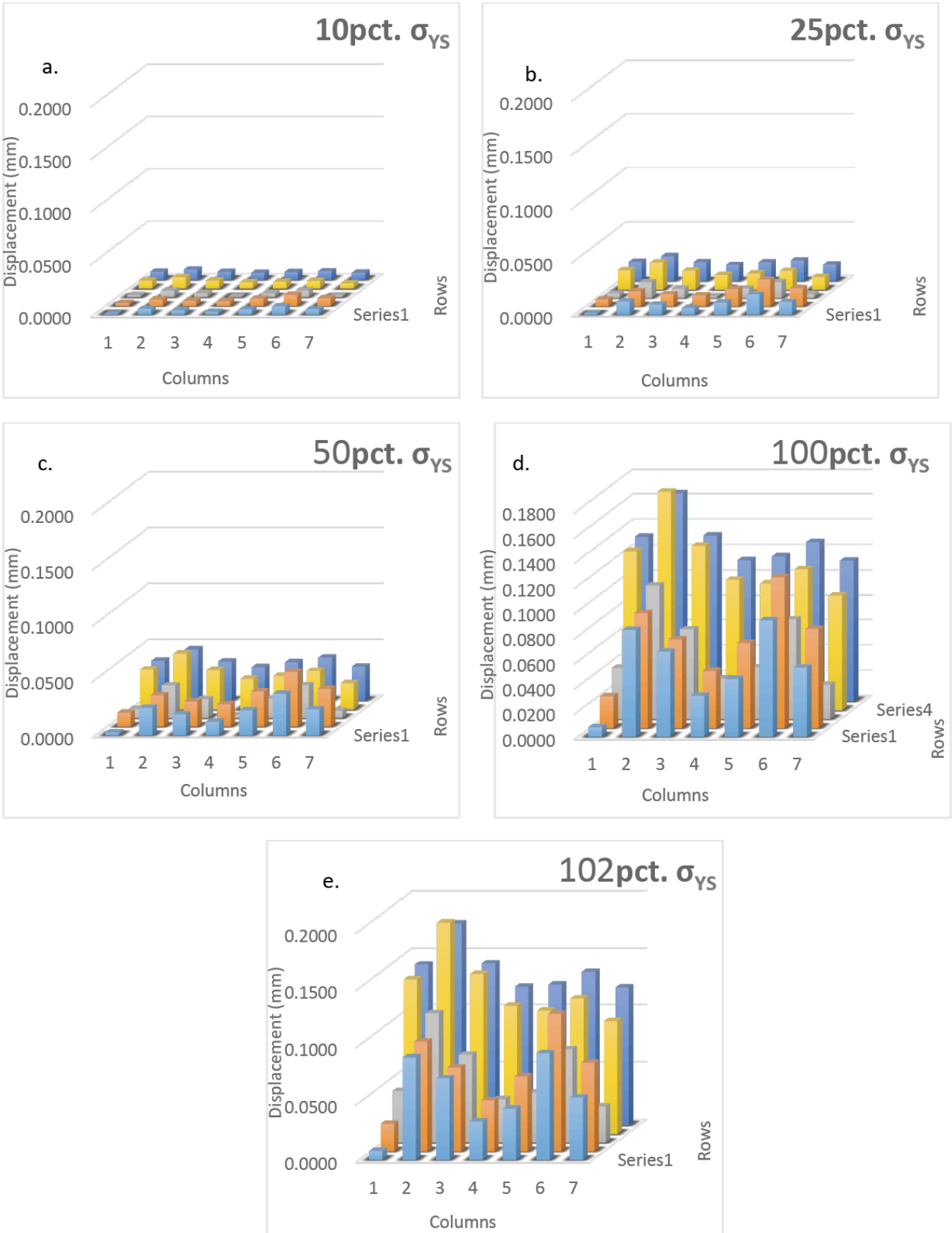


Figure 17: Profile showing the displacement experienced by the different nodes of the “thick” linked structure of carbon steel 1018 when subjected to symmetric loading, applied at Node (2, 6) and Node (4, 2). (a) 10 pct. of yield stress. (b) 25 pct. of yield stress. (c) 50 pct. of yield stress. (d) 100 pct. of yield stress. (e) 102 pct. of yield stress.

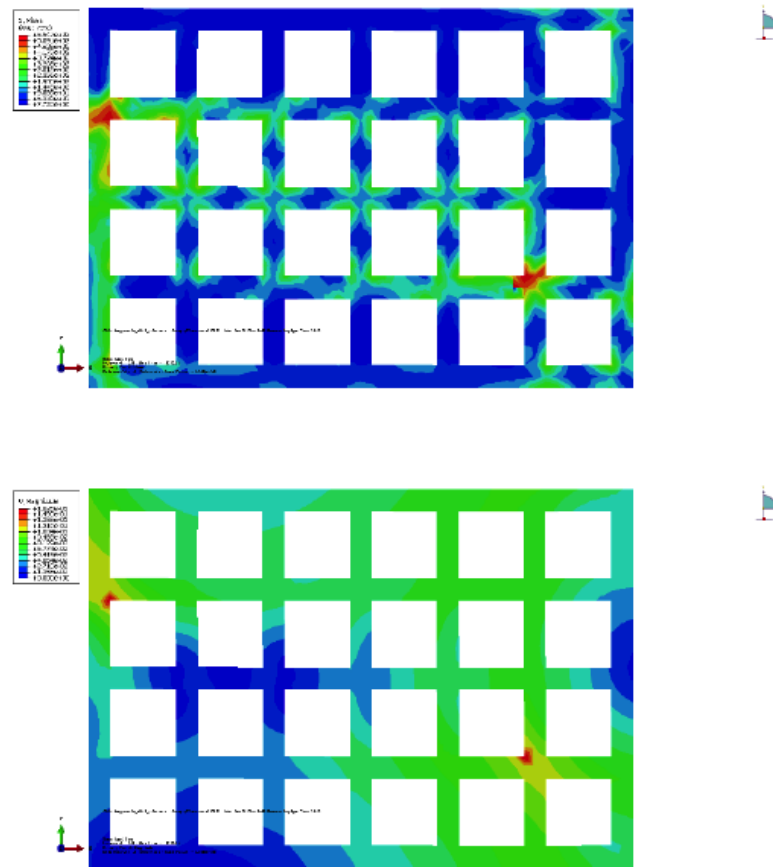


Figure 18(a): Profile showing the contours of the Von Mises stress for alloy steel 4140 that was subjected to asymmetric loading for Node (2,6) and Node (4,1) of the thick linked structure at load corresponding to yield stress of the chosen metal. **(b)** A contour profile showing the magnitude of displacements experienced by “thick” linked structure of alloy steel 4140 when subjected to asymmetric loading, 102 pct. of the yield stress.

[3, 4] under symmetric loading, starts to shift towards the right of the perforated metal plate. From the displacement data, it can be concluded that alloy steel 4140 provides a more uniform distribution for displacement experienced by the centroidal nodes when compared one-on-one with carbon steel 1018 containing a network of thick links.

For carbon steel 1018, a similar trend for the Von Mises stress having a higher concentration at the upper end of the metal structure was observed. This facilitates in the structure to begin yielding from and around the region of Node [1, 4] and the surrounding links. The Von Mises stress shown in the contour were much higher in numerical value when compared with alloy steel 4140 at identical values of the applied load, namely at 100 pct. of the yield load, and 102 pct. of yield load. The deformation experienced at the center of the structure containing a network of thick links was interesting since the stresses were initially low at Node

[3, 4] and upon gradual increase in the applied load, the centroidal nodes of the complete linked metal structure towards the right half experiences minimal deformation, which is different from the contours shown by alloy steel 4140 containing a network of thick links and subjected to asymmetric loading. Graphical representation of the numerical data is presented and discussed in detail elsewhere [23]. Overall, both the link elements and the nodal points experience low displacement on approximately 30 pct., of the perforated metal plate, with maximum impact occurring at the upper half of the perforated metal plate where pull by a tensile load is applied.

CONCLUSIONS

An analysis of the influence of thickness of the link elements, magnitude of the applied load as a function of the yield load, and nature of loading, i.e., symmetric versus asymmetric, on linked-metal structures of two

high strengths commercially used steels, following are the key findings:

1. Nature of loading, that is symmetric versus asymmetric, was observed to have minimal influence on stress versus strain behavior of a metal plate having an array of square perforations.
2. The Von-Mises failure criterion was used for purpose of analysis. An analysis of stresses and displacements experienced by the links and nodal points of a linked metal or perforated metal structure revealed plane stress conditions to prevail over a significant portion of the chosen perforated metal plate structure.
3. Numerical computation was used to obtain information pertinent to displacement and stresses developed in the link elements and displacements occurring or experienced by the nodal points or nodes in a metal structure that is essentially held together by a network of link elements of varying thickness and at the intersection of these elements are the nodes or nodal points. The displacement experienced by the links of carbon steel 1018 was noticeably higher than the displacement experienced by the links of alloy steel 4140.
4. Under the influence of an applied load, the values of both stress and displacement experienced by the links, or link elements, and the nodal points in a perforated metal plate were determined. The values of displacement experienced were higher for carbon steel 1018 when compared with values of alloy steel 4140. The stress distribution was essentially non-uniform through the linked metal structure of the two steels, with a higher or greater degree of stress concentration occurring at the corner of two intersecting links.
5. Two-dimensional [2-D] analysis was easy to perform for the case of both symmetric and asymmetric loading since it involved fewer calculations, i.e. less number of equations to solve the problem. An analysis of the 3-D model was not considered since thickness of the chosen metal plate is comparatively low when compared to other dimensions of the chosen metal plate.
6. Upon application of a given magnitude of load, as a fraction of yield load of the chosen metal, the values of displacement experienced by the link elements, or links, and the nodes dispersed through the linked metal structure were obtained. The value of displacement was observed to be noticeably different or non-uniform for both thick links and thin links and did give a definite shape when represented graphically on a 3-D bar graph.
7. The pattern shown by the displacement of the link elements of the two chosen steels was different depending on the nature of loading, symmetric versus asymmetric, for a specific magnitude of the load, as a function of the yield load, used.

REFERENCES

- [1] Jia S, Raiser GF and Povirk GL. Modeling the effects of hole distribution in perforated aluminum sheets I: Representative unit cells. *International Journal of Solids and Structures* 2002; 39: 2517-2532.
[https://doi.org/10.1016/S0020-7683\(02\)00115-4](https://doi.org/10.1016/S0020-7683(02)00115-4)
- [2] Yettram AL and Brown CJ. The elastic stability of square perforated plates under biaxial loading. *Computers and Structures* 22(4); 589-594.
[https://doi.org/10.1016/0045-7949\(86\)90010-6](https://doi.org/10.1016/0045-7949(86)90010-6)
- [3] Brown CJ and Yettram AL. The elastic stability of square perforated plates under combinations of bending, shear and direct loads. *Thin Walled Structures* 1986; 4: 239-246.
[https://doi.org/10.1016/0263-8231\(86\)90005-4](https://doi.org/10.1016/0263-8231(86)90005-4)
- [4] Brown CJ. Elastic buckling of perforated metal plates subjected to concentrated loads. *Computers and Structures* 1990; 36(6): 1103-1109.
[https://doi.org/10.1016/0045-7949\(90\)90218-Q](https://doi.org/10.1016/0045-7949(90)90218-Q)
- [5] Cirello Antonino, Furgiuele Franco, Maletta Carmine and Pasta Antonino. Numerical simulations and experimental measurements of stress intensity factor in perforated plates. *Engineering Fracture Mechanics* 2008; 75: 4383-4393.
<https://doi.org/10.1016/j.engfracmech.2008.05.007>
- [6] Vimal MN, Pridhar T, Viswanathan P and Subramanian R. Design and structural analysis of perforated sheet metals. *International Journal of Advanced Scientific and Technical Research* 2013; 4: 3.
- [7] Goldberg JE and Jabbour KN. Stresses and displacements in perforated plates. *Nuclear Structural Engineering* 1965; 2: 360-381.
[https://doi.org/10.1016/0369-5816\(65\)90055-4](https://doi.org/10.1016/0369-5816(65)90055-4)
- [8] Yettram AL and Awadalla ES. A direct matrix method for the elastic stability analysis of plates. *International Journal of Mechanical Sciences* 1968; 10(11): 887-901.
[https://doi.org/10.1016/0020-7403\(68\)90092-1](https://doi.org/10.1016/0020-7403(68)90092-1)
- [9] Fort PLE. Bending of Perforated plates with square penetration patterns. *Nuclear Engineering and Design* 1970; 12(1): 122-134.
[https://doi.org/10.1016/0029-5493\(70\)90138-X](https://doi.org/10.1016/0029-5493(70)90138-X)
- [10] Yettram AL and Brown CJ. The elastic stability of square perforated plates. *Computers and Structures* 21(6): 1267-1272.
[https://doi.org/10.1016/0045-7949\(85\)90180-4](https://doi.org/10.1016/0045-7949(85)90180-4)

- [11] Sirkis JS and Lim TJ. Displacement and strain measurement with automated grid methods. *Experimental Mechanics* 1991; 31(4): 382-388.
<https://doi.org/10.1007/BF02325997>
- [12] Chen FK. Analysis of plastic deformation for sheet metals with circular perforations. *Journal Materials Processing Technology* 1993; 37(1-4): 175-188.
[https://doi.org/10.1016/0924-0136\(93\)90089-O](https://doi.org/10.1016/0924-0136(93)90089-O)
- [13] Pedersen M, Olthuis W and Bergveld P. On The Electromechanical Behaviour Of Thin Perforated Backplates In Silicon Condenser Microphones. *Proceedings International Solid-State Sensors Actuators Conference - TRANSDUCERS* 1995; 95(2): 499-504.
<https://doi.org/10.1109/sensor.1995.721732>
- [14] Baik SC, Oh KH and Lee DN. Forming limit diagram of perforated sheet. *Scripta Metallurgica Materialia* 1995; 33(8): 1201-1207.
[https://doi.org/10.1016/0956-716X\(95\)00349-Z](https://doi.org/10.1016/0956-716X(95)00349-Z)
- [15] Webb DC, Kormi K and Al-Hassani STS. Use of FEM in performance assessment of perforated plates subject to general loading conditions. *International Journal of Pressure Vessel and Piping* 1995; 64(2): 137-152.
[https://doi.org/10.1016/0308-0161\(94\)00078-W](https://doi.org/10.1016/0308-0161(94)00078-W)
- [16] Huybrechts S and Tsai SW. Analysis and behavior of grid structures. *Composites Science and Technology* 1996; 56(9): 1001-1015.
[https://doi.org/10.1016/0266-3538\(96\)00063-2](https://doi.org/10.1016/0266-3538(96)00063-2)
- [17] Baik Seung Chul, Oh Kyu Hwan and Dong Nyung Lee. Analysis of the deformation of a perforated sheet under uniaxial tension. *Journal of Materials Processing Technology* 1996; 58(2-3): 139-144.
[https://doi.org/10.1016/0924-0136\(95\)02096-9](https://doi.org/10.1016/0924-0136(95)02096-9)
- [18] García-Garino C, Gabaldón F and Goicolea JM. Finite element simulation of the simple tension test in metals. *Finite Element Analysis Design* 2006; 42(13): 1187-1197.
<https://doi.org/10.1016/j.finel.2006.05.004>
- [19] Norris Jr DM, Moran B, Scudder JK and Qui-ones DF. A computer simulation of the tension test. *Journal of Mechanics and Physics of Solids* 1978; 26(1): 1-19.
[https://doi.org/10.1016/0022-5096\(78\)90010-8](https://doi.org/10.1016/0022-5096(78)90010-8)
- [20] Handbook, ASM Handbook, Volume 01 - Properties and Selection: Irons, Steels and High-Performance Alloys. ASM International, Materials ark, Ohio, USA 1990.
- [21] Prior AM. Applications of implicit and explicit finite element techniques to metal forming. *Journal Materials Processing Technology* 1994; 45(X): 649-656.
[https://doi.org/10.1016/0924-0136\(94\)90413-8](https://doi.org/10.1016/0924-0136(94)90413-8)
- [22] Abaqus / CAE User's Guide, Version 6.13.2, Dassault Systèmes, London, U.K.
- [23] Gargh Prashant P. *The Mechanical behavior of linked structures of four metals: Ferrous versus Non-ferrous: A numerical Study*. Master of Science Thesis, The University of Akron, Akron, Ohio, USA, August 2016.

Received on 16-09-2016

Accepted on 31-12-2016

Published on 01-06-2017

DOI: <http://dx.doi.org/10.15377/2409-9848.2017.04.01.03>© 2017 Gargh *et al.*; Avanti Publishers.

This is an open access article licensed under the terms of the Creative Commons Attribution Non-Commercial License (<http://creativecommons.org/licenses/by-nc/3.0/>) which permits unrestricted, non-commercial use, distribution and reproduction in any medium, provided the work is properly cited.